A&A 461, 115–119 (2007)
DOI: 10.1051/0004-6361:20064853

Astronomy & Astrophysics

Estimation of the detectability of optical orphan afterglows

Y. C. Zou[1], X. F. Wu[2,3], and Z. G. Dai[1]

[1] Department of Astronomy, Nanjing University, Nanjing 210093, PR China
e-mail: [zouyc;dzg]@nju.edu.cn
[2] Purple Mountain Observatory, Chinese Academy of Sciences, Nanjing 210008, PR China
e-mail: xfwu@pmo.ac.cn
[3] Joint Center for Particle, Nuclear Physics and Cosmology (J-CPNPC) between Nanjing University and Purple Mountain Observatory, Nanjing 210008, PR China

Received 13 January 2006 / Accepted 22 August 2006

ABSTRACT

Aims. By neglecting sideways expansion of gamma-ray burst (GRB) jets and assuming their half-opening angle distribution, we estimate the detectability of orphan optical afterglows.
Methods. This estimation is carried out by calculating the durations of off-axis optical afterglows whose flux density exceeds a certain observational limit.
Results. We show that the former assumption leads to more detectable orphans, while the latter suppresses the detectability strongly compared with the model with half-opening angle $\theta_j = 0.1$. We also considered the effects of other parameters, and find that the effects of the ejecta energy E_j and post-jet-break temporal index $-\alpha_2$ are important but that the effects of the electron-energy distribution index p, electron energy equipartition factor ϵ_e, and environment density n are insignificant. If E_j and α_2 are determined by other methods, one can constrain the half-opening angle distribution of jets by observing orphan afterglows. Adopting a set of "standard" parameters, the detectable rate of orphan afterglows is about 1.3×10^{-2} deg^{-2} yr^{-1}, if the observed limiting magnitude is 20 in R-band.

Key words. gamma rays: bursts

1. Introduction

Orphan afterglows are defined as afterglows whose gamma-ray bursts (GRBs) are not detected, possibly because of the Doppler effect for an off-axis observer. If the GRB afterglows are modelled perfectly, the observed rate of orphans and GRBs can be used to constrain the beaming factor of GRBs, as first proposed by Rhoads (1997). However, as many parameters are not determined well for different afterglows, it will be difficult to constrain the beaming factor tightly from optical orphans. Because late radio afterglows behave isotropic emission, the survey of radio afterglows may be helpful for estimating the beaming factor (Levinson et al. 2002; Gal-Yam et al. 2006), although one should be careful to rule out radio transients from other sources.

Other than constraining the beaming factor (Rhoads 1997; Dalal et al. 2002; Totani & Panaitescu 2002), some authors have focused on investigations of the detectability of orphan optical afterglows both theoretically (Nakar et al. 2002; Totani & Panaitescu 2002) and experimentally (Hudec 2004; Becker et al. 2004; Rykoff et al. 2005; Malacrino & Atteia 2006; Rau et al. 2006). Becker et al. (2004) give the results of a 5-year (1999–2004) survey of optical transients, but none was identified as an orphan. Rykoff et al. (2005) performed a 1.5-year survey (2003 September to 2005 March) of untriggered GRB afterglows. Although no orphan afterglow has been observed yet, they give the upper limit of the observed rate for a certain limiting magnitude. The surveys are still going on (Malacrino & Atteia 2006; Malacrino et al. 2006). On the theoretical side, Nakar et al. (2002) considered the following afterglow model: all jets propagating in a uniform medium (ISM) have a constant initial half-opening angle θ_j and a constant jet energy E_j. After a jet break takes place because the hydrodynamics of a sideways-expansion jet enters an exponential regime (Rhoads 1999; Sari et al. 1999), the temporal index of light curves becomes $-p$ (where p is the power-law index of shock-accelerated electrons). This decline is too steep for most of the observed late afterglows (Liang & Zhang 2005). On the other hand, many works (Moderski et al. 2000; Huang et al. 2000; Wei & Lu 2000; Salmonson 2003; Kumar & Granot 2003; Granot & Kumar 2003; Cannizzo et al. 2004) show that the sideways expansion of jets is insignificant at the relativistic stage. Thus, we consider relativistic jets without sideways expansion, and their afterglow light curves for an on-axis observer are shown in Fig. 1. The light curves are shown in the spherical case and the flux density $f_\nu \propto t^{-\alpha_1}$ when the Lorentz factor $\gamma > 1/\theta_j$. After the jet break time, the light curves steepen as $f_\nu \propto t^{-\alpha_2}$ ($\alpha_2 > \alpha_1$) because of the edge effect (Mészáros & Rees 1999), which is flatter than the sideways-expansion case. This will lead to more detectable orphan afterglows. A relationship between the jet break time and flux density ($f_{\nu,j} \propto t_j^{-p}$) was found by Wu et al. (2004) analytically and statistically.

Figure 1 is plotted based on the fact that the kinetic energies of all GRB jets have a similar value (Frail et al. 2001; Bloom et al. 2003). The statistical standard energy of jets has been discussed by several authors, e.g., Lipunov et al. (2001), and Panaitescu & Kumar (2002), who conclude that the collimation-corrected gamma-ray energy has a relatively narrow distribution, around 5×10^{50} erg. Berger et al. (2003) also obtained a standard kinetic energy reservoir of afterglows from the statistics on X-ray luminosity.

Recently, the distribution of the half-opening angle or viewing angle was investigated based on several structured-jet models

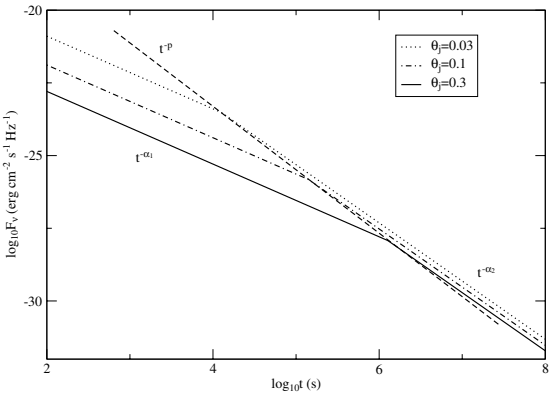

Fig. 1. Sketch of afterglow light curves from jets without sideways expansion for an on-axis observer. Dotted, dot-dashed and solid lines correspond to three jet opening angles 0.03, 0.1 and 0.3 respectively, with the same total kinetic energy $E_{\rm j} = 1 \times 10^{51}$ erg. The dashed line is the connection of jet breaks.

(Perna et al. 2003; Liang et al. 2004; Nakar et al. 2004; Guetta et al. 2005). Considering a uniform, sharp-edge jet (favored by Lamb et al. 2005), whose light curves are similar to those in the universal structured jet models (Rossi et al. 2002); and using the observed distribution of half-opening angles of the jets given by Lamb et al. (2005), one can derive the intrinsic distribution of $\theta_{\rm j}$, i.e., $P(\theta_{\rm j}) \propto \theta_{\rm j}^{-1}$ (see also Xu et al. 2005). We use this distribution as a weight for different opening angles as suggested by Guetta et al. (2005).

By considering both the effects of the constant half-opening angle during jet propagation and the distribution of initial jet half-opening angles, we here estimate the detectability of orphan afterglows and find that our results are different from the ones in earlier works (e.g. Nakar et al. 2002; Totani & Panaitescu 2002). We present the theoretical model in Sect. 2 and give the results of the detectability in Sect. 3. We summarize our findings and present a brief discussion in Sect. 4.

2. Theoretical analysis

We consider an adiabatic jet with a total kinetic energy $E_{\rm j}$ and a half-opening angle $\theta_{\rm j}$ and neglect sideways expansion. The hydrodynamics of the jet behaves as a spherical case (Sari et al. 1998). The Lorentz factor of the jet is given by

$$\gamma(t_\oplus) = 8.9(1+z)^{3/8} E_{\rm j,51}^{1/8} n_0^{-1/8} \theta_{\rm j,-1}^{-1/4} t_{\oplus,\rm d}^{-3/8}, \quad (1)$$

where z is the redshift of the GRB, n the number density of the interstellar medium (ISM), and $t_{\oplus,\rm d}$ the observed time in units of days. We adopt the conventional notation $Q = Q_k \times 10^k$ in this paper except for special explanations.

For an on-axis observer, there is a break in the light curve because of the edge effect (Mészáros & Rees 1999) when the bulk Lorentz factor γ equals $\theta_{\rm j}^{-1}$. The jet-break time is given by

$$t_{\rm j} = 0.82(1+z) E_{\rm j,51}^{1/3} n_0^{-1/3} \theta_{\rm j,-1}^2 \ \text{days}. \quad (2)$$

At the jet-break time, the flux density in the slow-cooling case ($\nu_{\rm m} < \nu < \nu_{\rm c}$) is (Wu et al. 2004)

$$F_{\nu,\rm j} = 515 t_{\rm j,day}^{-p} \times 50.2^{2.2-p} \kappa_{\rm f} \kappa_{\rm m}^{(p-1)/2} \epsilon_{\rm e,-1}^{p-1} \times \epsilon_{B,-3}^{(p+1)/4} \zeta_{1/6}^{p-1} n_0^{(3-p)/12} E_{\rm j,51}^{(p+3)/3} D_{L,28}^{-2} \times (1+z)^{(p+3)/2} \left(\frac{\nu}{\nu_R}\right)^{-(p-1)/2} \mu{\rm Jy}, \quad (3)$$

where $\kappa_{\rm m} = 0.73(p-0.67)$, $\kappa_{\rm f} = 0.09(p+0.14)$, and $\kappa_{\rm c} = (p-0.46)\exp(3.16-1.16p)$ are the correction factors (Granot & Sari 2002); $\epsilon_{\rm e}$ and ϵ_B are the energy equipartition factors of the electrons and magnetic field, respectively; $\zeta_{1/6} = 6(p-2)/(p-1)$; D_L is the luminosity distance; and $\nu_R = 4.55 \times 10^{14}$ Hz is the R-band frequency taken as the observed frequency. On the other hand, in the fast cooling case ($\nu_{\rm c} < \nu$), the flux density is (Wu et al. 2004)

$$F_{\nu,\rm j} = 3508 t_{\rm j,day}^{-p} \times 50.2^{2.2-p} \kappa_{\rm f} \kappa_{\rm m}^{(p-1)/2} \kappa_{\rm c}^{1/2} D_{L,28}^{-2} \times \epsilon_{\rm e,-1}^{p-1} \epsilon_{B,-3}^{(p-2)/4} \zeta_{1/6}^{p-1} E_{\rm j,51}^{(p+2)/3} n_0^{-(p+2)/12} \times (1+z)^{(p+2)/2} (1+Y_{\rm j})^{-1} \left(\frac{\nu}{\nu_R}\right)^{-p/2} \mu{\rm Jy}, \quad (4)$$

where $Y_{\rm j} = Y(t_{\rm j}) = (-1+\sqrt{1+4\eta\epsilon_{\rm e}/\epsilon_B})/2$ is the Compton parameter (Panaitescu & Kumar 2000; Sari & Esin 2001), and η is the radiation efficiency of electrons. Even though most GRB afterglows match the slow cooling case in the statistics by Wu et al. (2004), we here consider both fast and slow cooling cases, which are different from Nakar et al. (2002), who only considered the case $\nu > \nu_{\rm c} > \nu_{\rm m}$ for simplicity.

For an on-axis observer, the Lorentz factor of the jet $\gamma(t_\oplus)$ at earlier times ($t_\oplus < t_{\rm j}$) is greater than $\theta_{\rm j}^{-1}$, so the emission properties are the same as those from an isotropic fireball. The temporal decay index of the flux density $F_{\nu,0}(t_\oplus)$ is $(2-3p)/4$ in the fast cooling case and $3(1-p)/4$ in the slow cooling one (Sari et al. 1998). As index p is mainly in the range of $2.0 \sim 2.4$, we find that the range of the temporal index is about -0.7 to -1.3 for both cases, which is set to be a parameter $-\alpha_1$. When $t_\oplus > t_{\rm j}$ and if $\theta_{\rm j} \ll 1$ and $\gamma \gg 1$, the on-axis observer can only detect a fraction $\theta_{\rm j}^2\gamma^2$ of the flux density in the isotropic fireball case. As $\gamma(t_\oplus) \propto t_\oplus^{-3/8}$ (see Eq. (1)), the late decay index of the flux density $\alpha_2 = \alpha_1 + 3/4$.

For an off-axis observer with observing angle $\theta_{\rm obs}$, the time and frequency from on-axis (t_0, ν_0) and off-axis (t, ν) jets satisfy $t_0/t \simeq \nu/\nu_0 = (1-\beta)/(1-\beta\cos\theta_{\rm obs}) \equiv a$, where $\beta = \sqrt{1-1/\gamma^2}$ is the velocity in units of c; thus the flux density is

$$F_\nu(\theta_{\rm obs}, t) = a^3 F_{\nu/a}(0, at), \quad (5)$$

in the point source approximation, which is good enough when $\theta_{\rm obs} > \theta_{\rm j}$ (Granot et al. 2002).

Given a limiting flux density $f_{\nu,\rm lim}$ (corresponding to a limiting magnitude $m_{\rm lim}$) for an instrument with a fixed exposure time, we can calculate the detectable duration of an orphan afterglow: $t_{\rm obs}(z, \theta_{\rm obs}, \theta_{\rm j}, m_{\rm lim}) = t_{\rm max} - t_{\rm min}$, where $t_{\rm min}$ and $t_{\rm max}$ represent the earlier and later times when $F_{\nu,\theta_{\rm obs}} = F_{\nu,\rm lim}$. If the maximum observed flux density $F_{\nu,\theta_{\rm obs},\rm max} < F_{\nu,\rm lim}$, we take $t_{\rm obs} = 0$. Figure 2 shows the light curves of afterglows for different observing angles.

Following Nakar et al. (2002), we assume that the GRB rate $n(z)$ is proportional to the star formation rate (SFR), but we use a different SFR model as follows (Porciani & Madau 2001),

$$n(z) = B \frac{{\rm e}^{3.4z}}{{\rm e}^{3.4z}+22} \frac{\sqrt{\Omega_{\rm m}(1+z)^3+\Omega_\lambda}}{(1+z)^{1.5}} \quad (6)$$

where $\Omega_{\rm m}$ and Ω_λ are the cosmological parameters, and B the normalization factor. The parameter B satisfies $R_{\rm GRB}^{\rm true} = \bar{f}_{\rm b} R_{\rm GRB}^{\rm obs} = \int_0^{10} ({\rm d}V/{\rm d}z) n(z)/(1+z) {\rm d}z$, where $\bar{f}_{\rm b} = \int_{\theta_{\rm j,min}}^{\theta_{\rm j,max}} (1-\cos\theta_{\rm j})^{-1} P(\theta_{\rm j}) {\rm d}\theta_{\rm j} / \int_{\theta_{\rm j,min}}^{\theta_{\rm j,max}} P(\theta_{\rm j}) {\rm d}\theta_{\rm j}$ is the mean beaming factor of

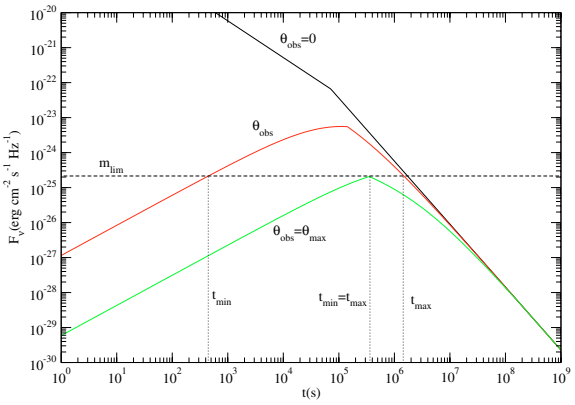

Fig. 2. Sketch for observations of orphan R-band afterglows. The three solid lines indicate the light curves with different observing angles. The one with $\theta_{\rm obs} = 0$ is not an orphan afterglow, which is plotted here as a reference. The horizontal dashed line represents a given limiting magnitude. The earliest and latest times ($t_{\rm min}$ and $t_{\rm max}$) at which an orphan afterglow are observed are represented by vertical dotted lines.

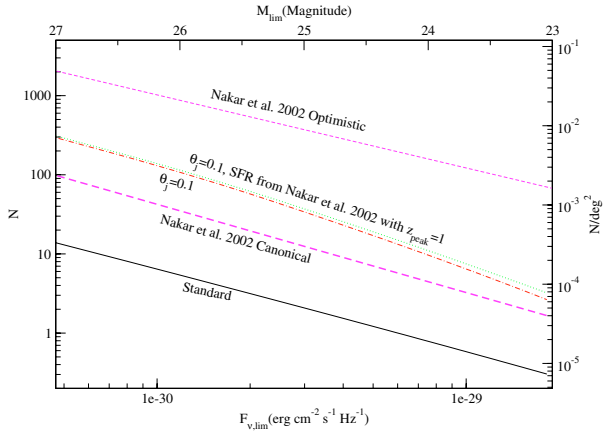

Fig. 3. The estimated number of orphan afterglows in a snapshot for the whole sky, as a function of the limiting flux density of detectors. The solid line represents our standard parameterized result, with $E_{\rm j} = 1 \times 10^{51}$ erg, $n = 1$ cm^{-3}, $p = 2.2$, $\alpha_2 = 1.8$, $\epsilon_{\rm e} = 0.1$, $\epsilon_B = 0.01$, $\nu = 4.55 \times 10^{14}$ Hz, and a power-law distribution of half-opening angles of the jets with $\theta_{\rm j,min} = 0.01$, $\theta_{\rm j,max} = 1$. The thick dashed line and the thin dashed line are respectively the canonical line and optimistic line in Nakar et al. (2002), who assumed a laterally spreading jet. The jets have fixed initial half-opening angles $\theta_{\rm j} = 0.1$ and 0.05. The dotted line denotes the same parameters as the canonical line in Nakar et al. (2002), but the assumption of no sideways expansion is used. The dot-dashed line is the same as the dotted one except for the SFR model in Porciani & Madau (2001).

GRBs and $R_{\rm GRB}^{\rm obs} = 667\ {\rm yr}^{-1}$ is the observed GRB rate. Here we assume all the GRBs can be observed if the observer is located within the solid angles of the jets and the redshift range is $0 < z < 10$.

If the exposure time is not too long (shorter than $t_{\rm obs}$), the number of detectable orphan afterglows in a single snapshot over the whole sky can be expressed as

$$N_{\rm orph} = \int_0^{10} \frac{n(z)}{(1+z)} \frac{{\rm d}V(z)}{{\rm d}z} {\rm d}z \int_{\theta_{\rm j,min}}^{\theta_{\rm j,max}} P(\theta_{\rm j}) {\rm d}\theta_{\rm j} \times \int_{\theta_{\rm j}}^{\theta_{\rm max}(z,m_{\rm lim})} t_{\rm obs}(z, \theta_{\rm obs}, \theta_{\rm j}, m_{\rm lim}) \theta_{\rm obs} {\rm d}\theta_{\rm obs}, \quad (7)$$

where $\theta_{\rm max}(z, m_{\rm lim})$ is the maximum observing angle, which satisfies $t_{\rm max}(\theta_{\rm max}) = t_{\rm min}(\theta_{\rm max})$, and $P(\theta_{\rm j})$ is the observational distribution function of half-opening angles of the jets with the upper and lower limits $\theta_{\rm j,max}$ and $\theta_{\rm j,min}$, which satisfies (Lamb et al. 2005)

$$P(\theta_{\rm j}) = \frac{\theta_{\rm j}^{-1}}{\ln(\theta_{\rm j,max}/\theta_{\rm j,min})}. \quad (8)$$

3. Numerical results

If the model parameters are given, the detectability of orphan afterglows can be estimated by Eq. (7). The main difference in detectability comes from the limiting magnitudes of detectors. Figure 3 shows the number of orphan afterglows that can be detected by one exposure on the whole sky. The solid line is the standard result, with parameters $E_{\rm j} = 1 \times 10^{51}$ erg, $n = 1$ cm^{-3}, $p = 2.2, \alpha_2 = 1.8, \epsilon_{\rm e} = 0.1, \epsilon_B = 0.01, \nu = 4.55 \times 10^{14}$ Hz, $\theta_{\rm j,min} = 0.01$, and $\theta_{\rm j,max} = 1$, where $E_{\rm j}, n, p, \epsilon_{\rm e}, \epsilon_B$, and ν are the same as in Nakar et al. (2002). As the pre-break temporal index of the optical light curve is about -1 (Zhang & Mészáros 2004), we choose $\alpha_2 = \alpha_1 + 3/4 \simeq 1.8$. The $\theta_{\rm min} = 0.01$ is adopted from Lamb et al. (2005). We take $\theta_{\rm max} = 1$, which does not influence the estimation significantly when we consider the distribution of half-opening angles of the jets. We also show the results of Nakar et al. (2002) in this figure with their canonical ($\theta_{\rm j} = 0.1$) and optimistic ($\theta_{\rm j} = 0.05$) parameters. For comparison, we plot the dotted line for a fixed half-opening angle $\theta_{\rm j} = 0.1$ and the SFR model in Nakar et al. (2002). One difference between the dotted line and the thick dashed line is the temporal index after the break time. We can see that the difference in detectability is due to the sideways expansion. Approximately, the flux density after the break time $t_{\rm j}$ is $F_\nu(t_\oplus) \simeq F_{\nu,{\rm j}}(t_\oplus/t_{\rm j})^{-p}$ in the sideways expansion case and $F_\nu(t_\oplus) \simeq F_{\nu,{\rm j}}(t_\oplus/t_{\rm j})^{-\alpha_2}$ in the non-sideways expansion case. Note that $F_{\nu,{\rm j}}$ and $t_{\rm j}$ have the same values in both cases, since the breaks both take place when $\gamma \simeq 1/\theta_{\rm j}$, and before the jet break time, both cases show isotropic evolutional behavior (Rhoads 1999; Mészáros & Rees 1999). Neglecting $t_{\rm min}$ and $\theta_{\rm j}$ in Eq. (7) and the potential influence of different spectra, we obtain the ratio of the detectabilities in the two cases (i.e., no sideways expansion vs. sideways expansion): $N_{\rm orph,NSE}/N_{\rm orph,SE} \simeq (F_{\nu,{\rm j}}/F_{\nu,{\rm lim}})^{11/(8\alpha_2)-3/(2p)}$. In general, if $\alpha_2 < p$, then $11/(8\alpha_2) > 3/(2p)$ and thus $N_{\rm orph,NSE} > N_{\rm orph,SE}$. For a larger limiting magnitude (i.e. smaller $F_{\nu,{\rm lim}}$), the ratio becomes higher. This is why in Fig. 3 the dotted line is higher than the thick dashed line for greater $m_{\rm lim}$. To show the effect of different SFR models, the dot-dashed line uses the SFR model in Nakar et al. (2002)[1] with $z_{\rm peak} = 1$, and the dotted line considers the SFR model in Eq. (6). These two lines are close to each other, which shows that the effect of the SFR models is insignificant. We note that the distribution of half-opening angles of the jets leads to further suppression of the detectability, which results in the difference between the dot-dashed and the solid lines. Combining the effects of the sideways expansion and distribution of the jet's half-opening angles, we obtain standard results (solid line in Fig. 3).

[1] The form of the SFR is

$$n(z) = B \begin{cases} 10^{0.75z} & z \le z_{\rm peak}, \\ 10^{0.75 z_{\rm peak}} & z > z_{\rm peak}, \end{cases}$$

where B is the normalization factor.

Table 1. The ratio of the number of orphan afterglows to the total number of afterglows for different limiting magnitudes of detectors. The values without and with brackets correspond to models A and B in Nakar et al. (2002) respectively to compare with their results.

$z_{\rm peak}$	$\theta_{\rm j}$	$m_{\rm lim}=23$	$m_{\rm lim}=25$	$m_{\rm lim}=27$
1	0.05	0.56(0.68)	0.73(0.78)	0.84(0.86)
1	0.10	0.33(0.39)	0.40(0.58)	0.63(0.71)
1	0.15	0.26(0.29)	0.34(0.40)	0.41(0.59)
2	0.10	0.22(0.36)	0.34(0.55)	0.60(0.70)

A more detailed comparison with Nakar et al. (2002) was performed and the results are listed in Table 1, which includes the ratio of the numbers of observable orphan afterglows to total observable afterglows. We choose the same SFR model (see Eq. (13) in Nakar et al. 2002), and the same model A and model B (i.e., the angle in Lorentz transformation $\theta = \theta_{\rm obs}$ for model A, and $\theta = \max(0, \theta_{\rm obs} - \theta_{\rm j})$ for model B), and neglect sideways expansion. We conclude that the ratios for model B are all higher than those for model A. Our ratios are somewhat lower than those in Nakar et al. (2002). This is because, for a fixed half-opening angle, the on-axis afterglow is brighter than in the sideways expansion case and the flux density of orphan afterglows does not increase very much, being due to the Doppler effect (see Eq. (5)).

Recently, Rykoff et al. (2005) performed a search for orphan afterglows, but none has been detected. They gave an upper limit for the observed rate $\eta_{\rm max} < 1.9$ deg^{-2} yr^{-1} by using the method suggested by Becker et al. (2004): $\eta = N/(\langle\varepsilon\rangle E)$ events deg^{-2} yr^{-1}, where N is the number of detected orphans, E the exposure, and $\langle\varepsilon\rangle$ the efficiency. Assuming a 30-min exposure time as in Rykoff et al. (2005), we obtain the exposure $E \simeq 2.35$ deg^2 yr for one whole sky survey. If the theoretical efficiency $\langle\epsilon\rangle$ is assumed to be unity, the observed rate is then $\eta \simeq 1.3 \times 10^{-2}$ deg^{-2} yr^{-1} and the detectability N is extrapolated to the 20th magnitude ($N \sim 0.03$) in the standard model. This is well below the upper limit 1.9 deg^{-2} yr^{-1} estimated by Rykoff et al. (2005) for the survey with limiting magnitude 20.

We also calculated the detectability for different parameters to show their effects. Figure 4 shows the detectability with different total kinetic energy $E_{\rm j}$. The solid line is the standard one, the same as the solid line in Fig. 3. If the value of $E_{\rm j}$ increases by one order of magnitude, the detectability increases by a factor of about 12. It is reasonable that N is greater for a higher kinetic energy. Generally speaking, the detectability is sensitive to the $E_{\rm j}$.

Figure 5 shows the detectability for different p and $\epsilon_{\rm e}$, with the solid line still the standard one. Remarkably, these parameters have minor effects on the results. Note that the p and α_2 are independent parameters here, unlike the sideways expansion case, where $\alpha_2 = p$ (Granot & Kumar 2003), so the variation in p does not change the temporal index α_2. The parameter p influences the flux density at time $t_{\rm j}$, which can be seen in Eqs. (3) and (4). The flux density is approximately proportional to $\epsilon_{\rm e}$, and the detectability is somewhat sensitive to $\epsilon_{\rm e}$. From those two equations, we can find that the other parameters n and ϵ_B do not significantly influence the detectability of optical orphan afterglows.

4. Discussions

We have calculated the number of orphan optical (R-band) afterglows that can be detected in an ideal survey of the whole sky with different limiting magnitudes. We considered jets without sideways expansion during the afterglow phase. This leads to a flatter light curve after the jet-break time $t_{\rm j}$, compared with the sideways-expansion case. Thus, orphan afterglows can persist for a longer time (above a certain flux density), and more expected orphans can be detected. The distribution of half-opening angles of jets was also considered, which suppresses the number of optical orphans compared with the case that all jets have one single half-opening angle $\theta_{\rm j} = 0.1$. When combining these two effects, the detectability is less than the canonical results of Nakar et al. (2002), who considered the case in which all jets have an initial half-opening angle $\theta_{\rm j} = 0.1$ with sideways expansion.

From Figs. 3–5, we can conclude that the main factors for the detectability are the total kinetic energy $E_{\rm j}$, half-opening angle of jet $\theta_{\rm j}$ and temporal index α_2. As $E_{\rm j}$ is considered to be a standard energy (Frail et al. 2001), our results can be used to constrain the value of the $E_{\rm j}$ by detecting orphans. If $E_{\rm j}$ and α_2 are determined accurately by other methods, the distribution function of the jet's half-opening angles can be determined well by observations of orphan afterglows.

However, our estimation is simplified in several aspects. First, the parameters are undetermined and diverse in different

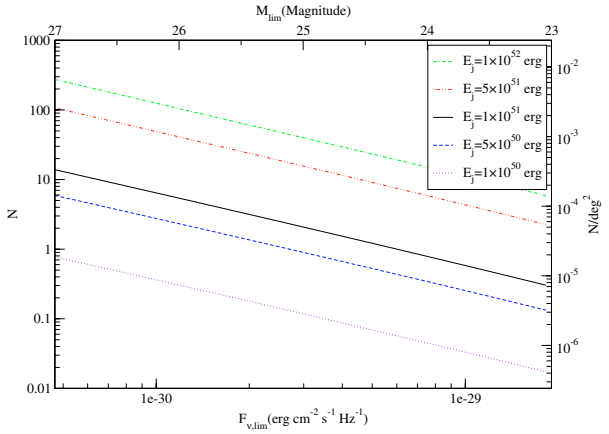

Fig. 4. Same as Fig. 3 with the standard parameters but for different total kinetic energies. From top to bottom, the $E_{\rm j}$s are 1.0×10^{52} erg, 5.0×10^{51} erg, 1.0×10^{51} erg, 5.0×10^{50} erg, and 1.0×10^{50} erg, while the solid line is the standard one.

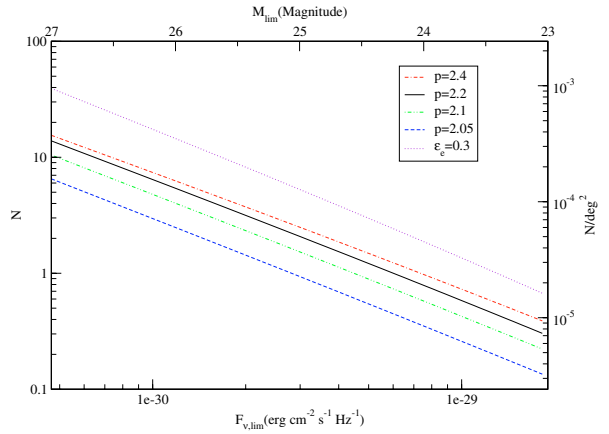

Fig. 5. Same as Fig. 3. The parameters are the same as the standard ones (solid line) but for $p = 2.4$ (the dot-dash-dashed line), $p = 2.1$ (the dot-dot-dashed line), $p = 2.05$ (the dashed line), and $\epsilon_{\rm e} = 0.3$ (the dotted line).

bursts. For a variable parameter, we should know its distribution. But this is very difficult. For example, the circum-burst environment seems to be an ISM, a wind, or another density-profile media, but these media cannot be determined clearly in well-observed GRBs. For simplicity, we choose the ISM with number density $n = 1$ cm^{-3}. Second, orphan afterglows may have properties similar to other phenomena: e.g., failed gamma-ray burst (Huang et al. 2002; Rhoads 2003; Huang et al. 2005) and "on-axis orphan afterglow" (Nakar & Piran 2003). Third, we use the model with a power-law distribution of half-opening angles of uniform jets. However, there are some other structured jet models that cannot be ruled out (Dai & Gou 2001; Rossi et al. 2002; Zhang & Mészáros 2002). These models also affect the detectability. Fourth, we assume that the GRB rate is proportional to the SFR, so our results are SFR-dependent. Fifth, when observing, one should distinguish orphan afterglows from other transients carefully (Levinson et al. 2002; Becker et al. 2004; Gal-Yam et al. 2006). Finally, the dust grains within the jet's opening solid angle may be evaporated by the prompt UV/X-ray photons, and the dust is possibly opaque in optical/UV bands outside the jet cone, so an optical orphan afterglow may be generally suppressed.

Acknowledgements. We would like to thank the anonymous referee and Steven N. Shore for valuable suggestions, and E. Nakar for helpful discussions. This work was supported by the National Natural Science Foundation of China (grants 10233010, 10221001, and 10503012). X.F.W. acknowledges the support from the China Postdoctoral Foundation, K. C. Wong Education Foundation (Hong Kong), and Postdoctoral Research Award of Jiangsu Province.

References

Becker, A. C., Wittman, D. M., Boeshaar, P. C., et al. 2004, ApJ, 611, 418
Berger, E., Kulkarni, S. R., & Frail, D. A. 2003, ApJ, 590, 379
Bloom, J. S., Frail, D. A., & Kulkarni, S. R. 2003, ApJ, 594, 674
Cannizzo, J. K., Gehrels, N., & Vishniac, E. T. 2004, ApJ, 601, 380
Dai, Z. G., & Gou, L. J. 2001, ApJ, 552, 72
Dalal, N., Griest, K., & Pruet, J. 2002, ApJ, 564, 209
Frail, D. A., Kulkarni, S. R., Sari, R., et al. 2001, ApJ, 562, L55
Gal-Yam, A., Ofek, E. O., Poznanski, D., et al. 2006, ApJ, 639, 331
Granot, J., & Sari, R. 2002, ApJ, 568, 820
Granot, J., & Kumar, P. 2003, ApJ, 591, 1086
Granot, J., Panaitescu, A., Kumar, P., & Woosley, S. E. 2002, ApJ, 570, L61
Guetta, D., Piran, T., & Waxman, E. 2005, ApJ, 619, 412
Huang, Y. F., Gou, L. J., Dai, Z. G., & Lu, T. 2000, ApJ, 543, 90
Huang, Y. F., Dai, Z. G., & Lu, T. 2002, MNRAS, 332, 735
Huang, Y. F., Lu, T., & Cheng, K. S. 2005, Ap&SS, 297, 53
Hudec, R. 2004, AIPC, 727, 240
Kumar, P., & Granot, J. 2003, ApJ, 591, 1075
Lamb, D. Q., Donaghy, T. Q., & Graziani, C. 2005, ApJ, 620, 355
Liang, E. W., & Zhang, B. 2006, ApJ, 638, L67
Liang, E. W., Wu, X. F., & Dai, Z. G. 2004, MNRAS, 354, 81
Lipunov, V. M., Postnov, K. A., & Prokhorov, M. E. 2001, Astron. Rep., 45, 236
Levinson, A., Ofek, E., Waxman, E., & Gal-Yam, A. 2002, ApJ, 576, 923
Malacrino, F., & Atteia, J.-L. 2006 [arXiv:astro-ph/0602370]
Malacrino, F., Atteia1, J.-L., Boër, M., et al. 2006 [arXiv:astro-ph/0605749]
Mészáros, P., & Rees, M. J. 1999, MNRAS, 306, L39
Moderski, R., Sikora, M., & Bulik, T. 2000, ApJ, 529, 151
Nakar, E., & Piran, T. 2003, New Astron., 8, 141
Nakar, E., Piran, T., & Granot, J. 2002, ApJ, 579, 699
Nakar, E., Granot, J., & Guetta, D. 2004, ApJ, 606, L37
Panaitescu, A., & Kumar, P. 2000, ApJ, 543, 66
Panaitescu, A., & Kumar, P. 2002, ApJ, 571, 779
Perna, R., Sari, R., & Frail, D. 2003, ApJ, 594, 379
Porciani, C., & Madau, P. 2001, ApJ, 548, 522
Rau, A., Greiner, J., & Schwarz, R. 2006, A&A, 449, 79
Rhoads, J. 1997, ApJ, 487, L1
Rhoads, J. 1999, ApJ, 525, 737
Rhoads, J. 2003, ApJ, 591, 1097
Rossi, E., Lazzati, D., & Rees, M. J. 2002, MNRAS, 332, 945
Rykoff, E. S., Aharonian, F., Akerlof, C. W., et al. 2005, ApJ, 631, 1032
Salmonson, J. D. 2003, ApJ, 592, 1002
Sari, R., & Esin, A. A. 2001, ApJ, 548, 787
Sari, R., Piran, T., & Narayan, R. 1998, ApJ, 497, L17
Sari, R., Piran, T., & Halpen 1999, ApJ, 519, L17
Totani, T., & Panaitescu, A. 2002, ApJ, 576, 120
Xu, L., Wu, X. F., & Dai, Z. G., 2005, ApJ, 634, 1155
Wei, D. M., & Lu, T. 2000, ApJ, 541, 203
Wu, X. F., Dai, Z. G., & Liang, E. W. 2004, ApJ, 615, 359
Zhang, B., & Mészáros, P. 2002, ApJ, 571, 876
Zhang, B., & Mészáros, P. 2004, IJMPA, 19, 2385